Přírodovědecká fakulta
Faculty of Science

Jihočeská univerzita v Českých Budějovicích
University of South Bohemia in České Budějovice

Bachelor Thesis

Counteracting constitutive activity of Orai1 with an H171Y mutation

Ricarda Marko

Supervisor: Mag.[a] Dr.[in] *Irene Frischauf MLBT*

Institute of Molecular Biophysics and Membrane biophysics, JKU

Ion channel group

České Budějovice 2021

Marko R., 2021: Investigation of changes in Pore structure upon addition of the H171Y mutant to ANSGA in Orai1. Bc. Thesis, in English – 28p, Faculty of Science, University of South Bohemia, České Budějovice, Czech Republic.

Annotation

The functions and structures of the Orai1-ANSGA mutation are still not completely known. To further investigate possible changes in pore structure, Orai1 ANSGA and H171Y in combination with different amino acids were used in cysteine-crosslinking studies, to see if the ANSGA and H171Y mutations affect the orientation of pore-lining residues.

Declaration

I hereby declare that I have worked on my bachelor's thesis independently and used only the sources listed in the bibliography.

I hereby declare that, in accordance with Article 47b of Act No. 111/1998 in the valid wording, I agree with the publication of my bachelor thesis, in full to be kept in the Faculty of Science archive, in electronic form in a publicly accessible part of the IS STAG database operated by the University of South Bohemia in České Budějovice accessible through its web pages. Further, I agree to the electronic publication of the comments of my supervisor and thesis opponents and the record of the proceedings and results of the thesis defense in accordance with aforementioned Act No. 111/1998. I also agree to the comparison of the text of my thesis with the Theses.cz thesis database operated by the National Registry of University Theses and a plagiarism detection system.

České Budějovice, 12.05.2021

Ricarda Marko

Acknowledgements

I would like to express my gratitude to my thesis supervisor, Mag.[a] Dr.[in] Irene Frischauf, MLBT, for guiding me through this project.

Further, I would like to thank Mario Janjić and Sascha Berlansky for the help and instructions they provided and for creating a comfortable working environment.

I want to thank Univ.-Prof. Dr. Christoph Romanin for giving me the opportunity to work on my bachelor thesis in his laboratory.

I would like to acknowledge Prof. RNDr. Libor Grubhoffer, CSc. and Univ.-Prof. Dr. Norbert Müller for the establishment and management of the Biological Chemistry Program.

Also, I would like to thank my family for having a lot of patience with me and my studying progress over the years.

Lastly, I would again like to thank Mag.[a] Dr.[in] Irene Frischauf, MLBT and RNDr. Ján Štěrba, Ph.D. for finally making this Thesis possible despite all the obstacles.

Abstract

Orai1 is the pore-forming subunit of the Calcium release activated Ca^{2+} (CRAC) channel in the plasma membrane of excitable and non-excitable cells. By interaction of the ER-resident STIM1 protein with ORAI1, CRAC channels are activated and internal Ca^{2+} stores are refilled. Previous research has shown that using a gain-of function mutation in Orai1 (ANSGA) the channel acquires a constitutively open conformation. (Lunz et al., 2019) H171Y is believed to act as a break-mutation, abolishing the constitutive activity of the ANSGA mutant (unpublished data). To further investigate changes in pore structure that occur due to channel opening, ANSGA and H171Y in Orai1 in combination with different mutations in pore-lining amino acids were used in cysteine-crosslinking studies. Possible changes in channel conformation can then be observed using Western Blot and immunodetection with suitable antibodies, which were used to visualize the formation of disulphide bridges in the form of dimers. Contrary to what has been assumed, the ANSGA mutation in combination with certain amino acids that were used in our study, did lead to a change in pore structure, but did not always cause the expected dilation of the pore (which indicates a constitutively open channel conformation) but rather led to close proximity (and thus a more closed channel conformation) at the specific residue. By addition of the H171Y this could in most cases be reversed.

Table of content

Abbreviations

NMDA	N-methyl-D-aspartamereceptors
VM	Voltage-gated channels
HVA	High voltage activated / High-threshold
LVA	Low voltage activated / Low-threshold
VGCC	Voltage-gated Ca^{2+} channels
SOC	Store operated channels
IP3R	Inositol (1,4,5)-triphosphate receptor
InsP3	Inositol (1,4,5)-triphosphate
CIF	Ca^{2+}-influx factor
TRPC	Transient receptor potential channels
ER	Endoplasmic Reticulum
SR	Sarcoplasmic reticulum
GCR	G protein-coupled receptor
RTK	Receptor tyrosine kinases
SERCA	Sarcoendoplasmic reticular Ca^{2+} ATPase
ATP	Adenosintriphosphate
PMCA	Plasma membrane Ca^{2+} ATPase
CRAC	Ca^{2+} release activated Ca^{2+} channels
STIM1	Stromal interaction molecule1
PM	Plasma membrane
PLC	Phospholipase C
TM	Transmembrane
SERCA	Sarco(endo)plasmic reticulum Ca^{2+}-ATPase
WT	Wild type
HEK	Human embryonic kidney
HRP	Horseradish peroxidase
ETON	Extended transmembrane Orai1 N-terminal
ANSGA	four-point mutation in hinge region aa position 261–265

1. Introduction

1.1. Ion channels

"Ion channels are protein molecules that span across the cell membrane allowing the passage of ions from one side of the membrane to another (Baker et al., 2017)." By shifting between closed and open conformational states, the conductive pathway is 'gated', meaning they control the passive ion flow through the plasma membrane. This conformational transition can be driven by V_M, ligand binding or other mechanisms such as membrane stretch (mechanically-gated channels). If the stimulus is removed, the channels close. If the activating factor persists, most channels progressively reach a closed state, by a process called inactivation or desensitization. Removing the stimulus after inactivation or desensitization has already taken place, the channels can't be immediately reactivated by further stimulus application (Di Resta & Becchetti, 2010). Once the ion channels are opened, they show a selectivity for the ions that are allowed to pass through them. There are some channels that only allow specific ions to pass through; for example, Sodium (Na^+) channels only allow Na^+ ions to pass through. Other channels allow broader groups, for example, NMDA allow Na^+, Ca^{2+} and K^+ to pass through them (Baker et al., 2017). No ion channel is perfectly selective (Di Resta & Becchetti, 2010).

1.2. Ca^{2+} Channels and Ca^{2+} signalling

Intracellular Ca^{2+} is the most common signal transduction element in cells but cannot be metabolized like other second-messenger molecules (Clapham, 2007). Its concentration controls numerous processes; for example, gene expression and transcription, cell signalling, neurotransmitter and secretion release, (Baker et al., 2017) cardiac and smooth muscle contraction, (Di Resta & Becchetti, 2010) learning and memory (Baker et al., 2017). Although it is necessary for life, a prolonged high intracellular Ca^{2+} level leads to cell death. Normal intracellular Ca^{2+} concentration is around 100mM (Clapham, 2007). Ca^{2+} signalling functions by generating brief pulses of Ca^{2+} with various on/off reactions. The signal is either derived from internal stores (usually ER or SR), which is controlled by Ca^{2+} itself or by an expanding group of messengers, or from external medium, via various types of plasma-membrane channels (Berridge et al., 2003). The ER actively secludes Ca^{2+} into its intraorganellar space via Ca^{2+} pumps (SERCA pumps), ATP and specialized buffer molecules such as calsequestrin. PMCA (plasma membrane Ca^{2+} ATPases) pumps are responsible for pushing the Ca^{2+} out of

the cell. ATPases exchange protons for two (SERCA) or one (PMCA) Ca^{2+} per ATP hydrolysed (Clapham, 2007). The basic reactions are outlined in Figure 1 (Berridge et al., 2003).

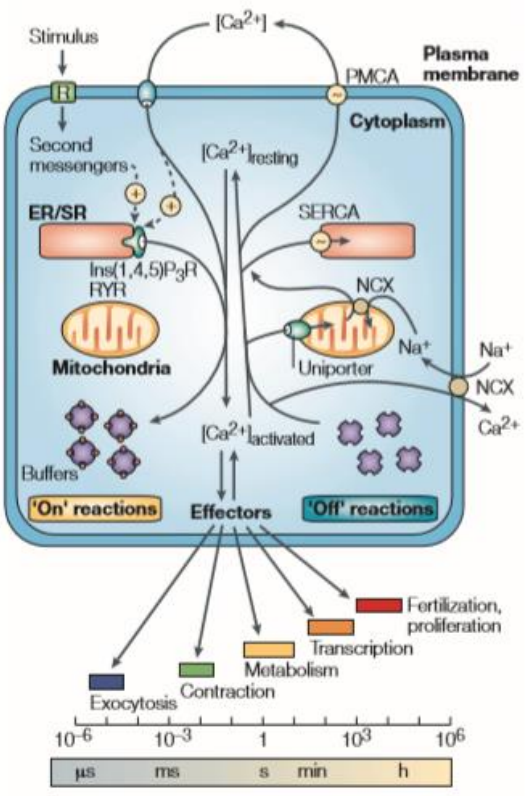

Figure 1: ***Calcium signalling dynamics and homeostasis. (Berridge et al., 2003)***

During 'on' reactions, entry of external Ca^{2+} and the formation of second messengers that release internal Ca^{2+} (stored in the ER), is induced. Most of the Ca^{2+} is bound to buffers, while a small proportion binds to the effectors that activate various cellular processes. During the 'off' reactions, Ca^{2+} leaves the effectors and buffers and is removed from the cell. The Na^{+}/Ca^{2+} exchanger (NCX) and the plasma-membrane Ca^{2+}-ATPase (PMCA) extrude Ca^{2+} to the outside, then the Ca^{2+} is pumped back into the ER with SERCA. Mitochondria actively sequester Ca^{2+} rapidly through a uniporter during the recovery process, it is then released more slowly back into the cytosol for further interaction with the SERCA and the PMCA. Ca^{2+} fluxes during the off reactions exactly match those during the on reactions. $[Ca^{2+}]$ (Berridge et al., 2003).

1.3. Voltage gated Ca^{2+} channels

In excitable cells, the main pathway for Ca^{2+} influx is via highly selective voltage gated Ca^{2+} channels (VGCC) (Nowycky, 2002). Voltage-gated Ca^{2+} channels are activated by membrane depolarization (Di Resta & Becchetti, 2010). Ca^{2+} channels, although they have a common molecular structure, are divided into two main families. High voltage-activated (HVA), (Baker et al., 2017) which activate around -30 mV and produce steady currents, with slow inactivation, (Di Resta & Becchetti, 2010) and low voltage-activated (LVA), (Baker et al., 2017) which activate around -60mV and which present a much quicker interaction, (Di Resta & Becchetti, 2010) calcium channels, which can be seen in Figure 1.

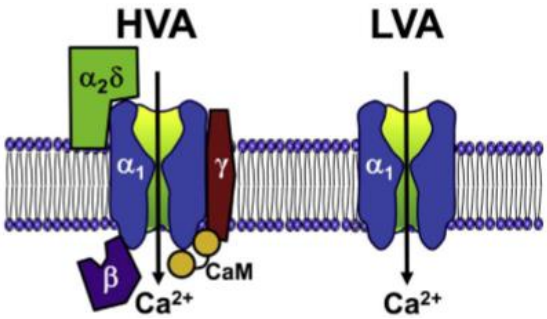

Figure 2: ***Topology of HVA and LVA voltage-gated Ca^{2+} channels. (Baker et al., 2017)***

The types of Ca^{2+} channels are further differenced into four major types, called T, L, N and P. LVAs (T-type) are temporarily activated by relatively small depolarizations from hyperpolarized holding potentials and are inactivated at positive potentials. HVAs (L, N, P-types) are activated at more positive potentials and display diverse kinetic properties (Snutch & Reiner, 1992).

The Ca_v α-subunit represents the main pore-forming Ca^{2+} channel subunit. Subunits are arranged in a 24 transmembrane protein and divided into four homologous domains (I-IV), with each six transmembrane segments (S1-S6) and intracellular N- and C-termini (Baker et al., 2017). The S4 segments act as specialized voltage-sensing regions. By depolarization from the resting membrane potential (~70mV), (Clapham, 2007) each segment undergoes a rotating movement, thus initiating the overall conformational change and allowing the pore channel to open. The S5 and S6 segments form loops which line the inside of the pore and determine ion conductance and selectivity. Ca^{2+} ion selectivity is determined by a pair of glutamine residue on each segment and is unique to Ca^{2+} channels (Baker et al., 2017).

1.4. Voltage independent Ca^{2+} channels

In nonexcitable cells, (Clapham, 2007) Ligand-gated ionotropic (Voltage-independent) channels represent the most numerous and varied Ca^{2+}-influx pathways and are relatively non-selective for cations and can pass large amounts of Ca^{2+}. Inside the organelles, the ions are bound to specialized Ca^{2+} buffering proteins (Nowycky, 2002), which can be either mobile or immobile (Clapham, 2007). Store operated channels (SOC) are regulated by the level of free Ca^{2+} in the lumen of the ER (Prakriya, 2009). They open in response to Ca^{2+} release from the ER lumen into the cytoplasm after receptor activation (Lunz et al., 2019). Mechanism of activation can be the interaction with IP_3R, a diffusible Ca^{2+}-influx factor (CIF) or channel insertion into the membrane (Nowycky, 2002). IP_3R binds to specialized tetrameric $InsP_3$ receptors that span the ER membrane and trigger the release of Ca^{2+} from the ER. The $InsP_3$ is released by two receptor classes; the GCRs and the RTKs (Clapham, 2007). Ca^{2+} release activated channels (CRAC) are highly selective and found in the blood lineage. Whereas TRPC are mostly nonspecific cation channels, which indirectly respond to hormones and transmitters through phospholipase Cß activation and via second messengers (Nowycky, 2002).

1.5. CRAC channels

The CRAC channels are the best characterized SOCs and have two key players: STIM1 and Orai1 (Lunz et al., 2019). There are at least ~10.000 functional CRAC channels expressed (Parekh, 2010) in T cells, mast cells and other tissues and regulate critical cellular processes. In the absence of selective inhibitors, CRAC channels are involved in T-cell activation and essential for gene transcription. CRAC channels contain an intrapore Ca^{2+} binding site, from which the high selectivity arises (Prakriya, 2009). CRAC channels are activated by a fall in Ca^{2+} levels within the ER store, regardless of how the stores are consumed. Although they are not voltage activated, a change in the membrane potential affects the driving force for Ca^{2+} flux through the channels (Parekh, 2010).

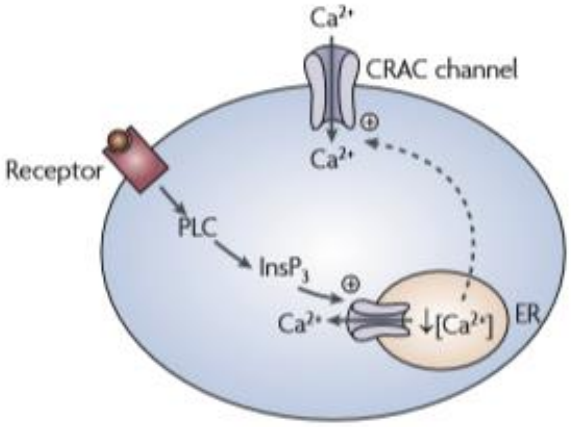

Figure 3: ***Schematic store operated calcium entry in CRAC. (Parekh, 2010)***

A fall in Ca^{2+} concentration in the ER, triggers cell-surface receptors to activate the enzyme PLC and cause an increase in $InsP_3$. This leads to an opening of the CRAC channels in the PM and thus to an increase in Ca^{2+} levels. A fall in concentration is sensed by STIM1, which relays this signal to ORAI1 in the plasma membrane (Parekh, 2010).

1.6. STIM1

STIM1 is a 77 kDa single-pass transmembrane protein (Prakriya, 2009) with no known catalytic activity (Parekh, 2010) and acts as a Ca^{2+} sensor in the ER. Its N-terminus is located inside the ER lumen, followed by a single TM spanning domain and a cytosolic C-terminus (Lunz et al., 2019). It is expressed in nearly all mammalian tissues (Prakriya, 2009) and shows constitutive movement along microtubules within the ER, in resting cells, with replete Ca^{2+} stores (Lunz et al., 2019). A missense mutation in the STIM1 exon 7 can cause Stormorken syndrome, which is an autosomal-dominant disease (Misceo et al., 2014). Dominant STIM1 mutations can also be a genetic cause of tubular aggregate myopathy that can lead to several muscle disorders such as exercise-induced cramps or inherited myasthenia (Möhm et al., 2013). ER Ca^{2+} store-depletion induces a dissociation of bound Ca^{2+} ions from the luminal EF hand of STIM1 (Lunz et al., 2019) and causes the exposed hydrophobic SAM domains to form homotypic interactions with each other and therefore initiates STIM1 oligomerisation (Parekh, 2010) and translocation (Lunz et al., 2019) from the bulk ER into puncta near the plasma membrane (Prakriya, 2009). A signal, which is transduced through the TM segment, reaches the cytosolic coiled-coil domains and causes a higher order STIM1 oligomerization. The EF

hand exhibits a helix-loop-helix motif with negatively charged aspartates and glutamates that interact with Ca^{2+} as long as the Ca^{2+} concentration in the ER is high (Lunz et al., 2019).

EF-hand mutations mimic the store-depleted state, which disables STIM1 to bind Ca^{2+} (Lunz et al., 2019). This causes the cells to show CRAC channel opening without store depletion, (Prakriya, 2009) which is of advantage when examining ER lumen-to-cytosol signal transduction (Lunz et al., 2019).

The STIM C-terminus is composed of 3 coiled-coil regions, a CRAC modulatory domain, (Lunz et al., 2019) which includes the STIM1 homomerization domain, followed by a serine/proline and a polybasic lysine-rich region. The lysine region at the end of the C-terminus binds to membrane phospholipids and anchors STIM1 to its target (Rosado et al., 2016). This C-terminus is sufficient to activating CRAC currents through Orai1 (Lunz et al., 2019). The CC-regions are highly conserved but have an inequality in their function (Rosado et al., 2016). Several cytosolic STIM1 fragments are capable to activate Orai1: OASF, SOAR, CAD and CCb9 (Lunz et al., 2019). CC2 and CC3 domain comprise the SOAR domain, (Rosado et al., 2016) which exhibits an R-shaped structure that can be seen in figure 4 (Lunz et al., 2019).

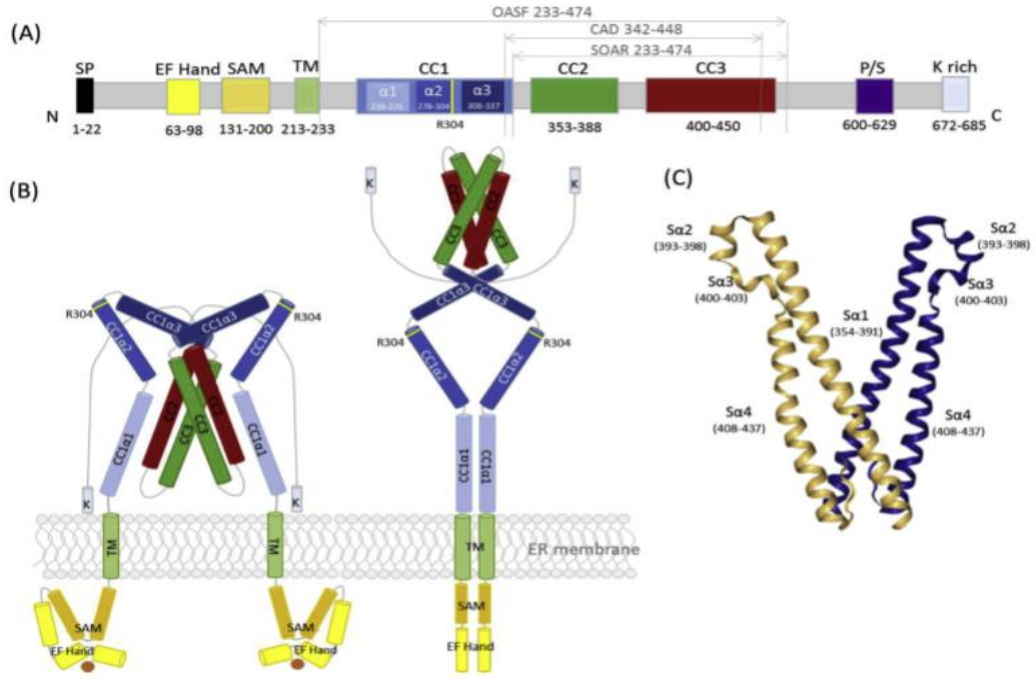

Figure 4: ***(A)*** *Schematic representation of full length human STIM1 including essential regions and overall structure.* ***(B)*** *STIM1 model in the resting (left) and activated (right) state.* ***(C)*** *STIM1 SOAR domain depicting Sα1-4 regions (Lunz et al., 2019).*

Besides STIM1, there is another mammalian homolog of STIM, called STIM2. It is an 84 kDa protein that mediates Orai1 channel activation under resting conditions, when the agonist stimulation is absent. It has a weaker Ca^{2+} binding affinity than STIM1 and induces a weaker activation of Orai1 (Lunz et al., 2019).

1.7. Orai1/CRACM1

Orai1 accumulates at the opposite sites of STIM1 and is the pore-forming subunit of the CRAC channel in the PM. This allows for direct interaction between STIM1 and Orai1 and leads to CRAC channel activation and thus refilling of internal Ca^{2+} stores (Lunz et al., 2019). Orai channels contain three conserved homologs (Rosado et al., 2016) in mammals: Orai 1-3. Each Orai forms a hexameric channel complex with a highly selective Ca^{2+} pore in the PM. Orai1 is a 33 kDa protein with four transmembrane domains (Lunz et al., 2019). Two loops are exposed to the extracellular medium, and one loop and the N- and C- termini facing the cytoplasm, (Rosado et al., 2016) which can be seen in figure 5.

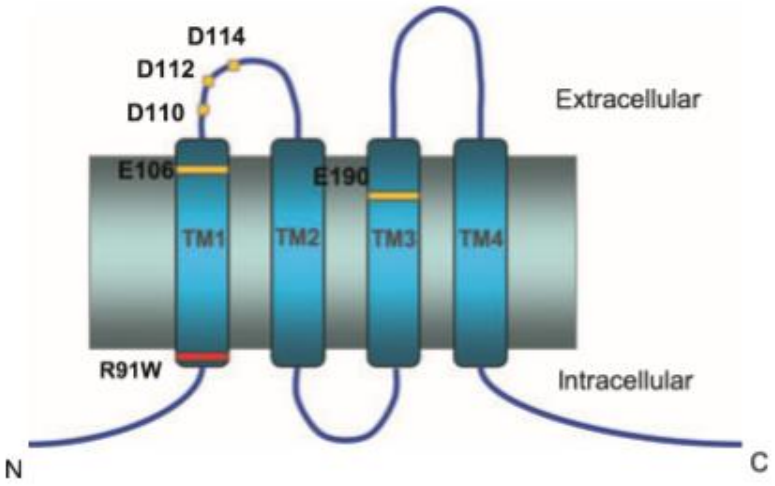

Figure 5: ***Predicted topology of Orai1 (Prakriya, 2009).***

Both termini are required for STIM1 interaction and regulation (Rosado et al., 2016). The C-termini of the TM4 helices are arranged in pairs, bending in opposite directions to form coiled-coil interactions with other Orai subunits. A gain-of function mutation (dOrai H206 A corresponding to hOrai1 H134 A) can cause the channel to switch into a constitutively open conformation (Lunz et al., 2019). Orai channels can also form heteropentamers to function as arachidonate-regulated Ca^{2+} channels, which are store-independent channels, regulated by PM_resident STIM1 (Rosado et al., 2016).

1.8. Orai1-ANSGA

A five amino-acid segment in human Orai1 (LVSHK), which is called the ‘nexus’, links the C-terminal STIM-binding helical extension of TM4 to the TM3 helix. Through the nexus, information from the external STIM-binding site is transmitted to the core of the channel to mediate channel gating. This nexus channel can also mutate to ANSGA that mimics the conformational change of the TM4-ext caused by STIM1-binding (Zhou et al., 2017). Orai-ANSGA, which is highly constitutively active, and the less-active Orai1-ANSHK channel derivatives, are expressed in HEK cells, exclusively localized to the PM. Both channels give large constitutive Ca^{2+} inward currents. The Orai1-ANSGA mutant mediates authentic, constitutive I_{CRAC}, which cannot be distinguished from CRAC current mediated by Orai1-WT in response to STIM1. Orai1-ANSGA is fully active, it has maximal constitutive I_{CRAC} at break-in and no further current development after store depletion (Zhou et al., 2016).

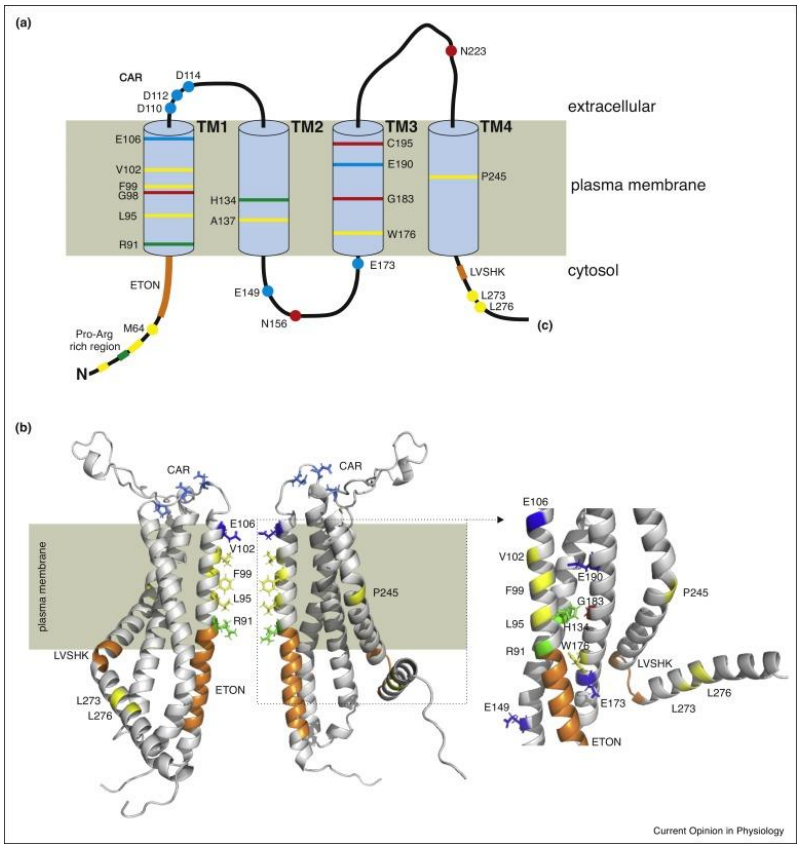

Figure 6: ***Schematic and structural representation of important domains in Orai1 proteins. (Sallinger et al., 2020)***

Figure 6, (a) shows a schematic representation of an hOrai1 monomer. The important regions as well as amino acids are highlighted. Inside the cytosol with a range from aa1-91 and aa259-301 are the N-termini and the C-termini located. The region of aa73-90 is called

the ETON (extended transmembrane Orai1 N-terminal) region, which is involved in STIM1/Orai1 activation and is highlighted in orange. The four TM-domains at aa92-106, aa118-140, aa174-197 and 236-258 are connected via extracellular (loop 1 and 3) or intracellular loops (loop 2). The yellow highlighted areas represent important unipolar horai1 residues and domains, while green are basic, blue acidic and red show neutral/polar side chains.

In Figure 6, (b) a cross section 3D model of a hexameric hOrai1 channel is displayed by two hOrai1 monomers facing each other with TM2-TM4 for stabilizing the pore-forming TM1-helices. The side chains of residues within the TM2-TM3, which are crucial for TM domain stability are depicted on the right, while side chains of amino acid residues facing the ion-conducting pore are shown on the left. (Sallinger et al. 2020)

2. Aims

- Introduction of H171Y into an Orai1 ANSGA construct to abolish its constitutive activity.
- Construction of cysteine-crosslinking experiments to probe what influence ANSGA and H171Y-ANSGA have on the pore structure of Orai1.
- Substitution of the positively charged histidine residue at position 171 with a negative residue, should cause deformation of the pore structure and pore-leakage.
- Investigation of the channel opening by introducing ANSGA in a H171Y plasmid and other pore-lining amino acid mutant (R191C, F99C, etc.), to see if a change in dimerization can be observed.

3. Methods

3.1 Insertion of point mutations and Amplification via PCR

The primers used for PCR are listed in Table 1. The reagents for obtaining 45.5 µl of PCR mastermix are seen in Table 2. The cycling conditions (Table 3) were set according to the manufacturer's instructions and primer melting temperatures. In addition, one negative control, containing no template DNA or Polymerase was prepared.

Table 1: PCR primers (ordered from Eurofins Genomics)

gene	forward primer	reverse primer
H171Y	5'-caggccagctcgatatagcggtgcatgcgct-3'	5'-agcgcatgcaccgctatatcgagctggcctg-3'
R91C	5'-gagcagagccgaggtgcagctggaggctttaag-3'	5'-cttaaagcctccagctgcacctcggctctgctc-3'
F99C	5'-accatggcgcagccggagagcagagcc-3'	5'-ggctctgctctccggctgcgccatggt-3'
E106C	5'-cagcgtccagctgcacgcacaccattgccaccatg-3'	5'-catggtggcaatggtgtgcgtgcagctggacgctg-3'
ANSGA	5'-gctcctggaactgtcggtcagtcgcaccgctattcgctgagcggtagaagtggacggcga-3'	5'-tcgccgtccacttctaccgctcagcgaatagcggtgcgactgaccgacagttccaggagc-3'

Table 2: PCR reaction mixture

reagent	[stock]	volume
H_2O (nuclease free)		37.05µl
DMSO		1.5µl
dNTPs (10mM)		1.5µl
Forward primer (125ng)		1.25µl
Reverse primer (125ng)		1.25µl
Template DNA (between 10-100ng)		1µl
PFU-Polymerase (1U)		1µl
PFU-Polymerase buffer (10x)		5µl

Table 3: PCR cycling conditions

step	temperature	time	cycles
Polymerase activation	**90°C**	**2 min**	**1**
Denaturing	**95°C**	**40 sec**	
Annealing	**60°C**	**40 sec**	**18**
Extension	**68°C**	**8 min**	
elongation	**68°C**	**10 min**	**1**
cooling	**4°C**	**-**	**-**

After performing the PCR according to protocol, an agarose-gel electrophoresis was performed, as seen in figure 7. A 15 µl aliquot of each undigested PCR product was mixed with 7 µl loading dye and run on 1% agarose gel in 1xTAE electrophoresis buffer (composition of TAE buffer in Table 4). The gel was prepared by dissolving 1.5g agarose in 150ml 1x TAE buffer. Two different markers were used for the gel electrophoresis. The first marker used was Lambda-HindIII marker (left), the second one was Bechtop 100bp marker (right), both purchased from the company Promega. The electrophoresis was performed at 100V for approximately 25 minutes and was subsequently analyzed in UV-Light with Bio-Rad UV Gel Imager.

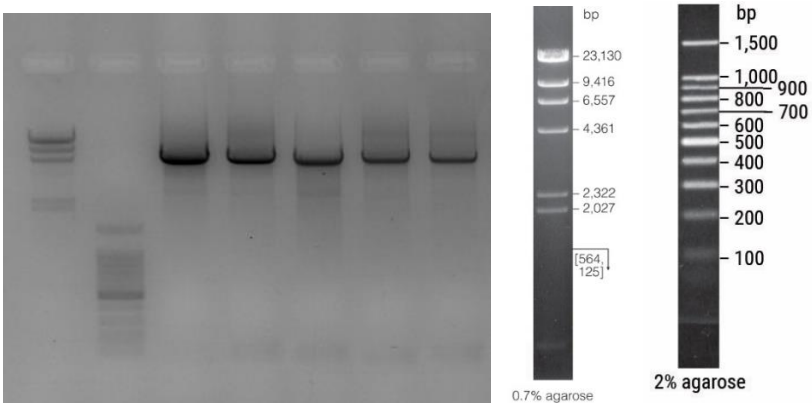

Figure 7: ***Typical result of an agarose-gel electrophoresis after a point mutation***

Table 4: 50x TAE buffer (1L)

R**eagent**	**final**
T**ris Base**	**2M**
E**isessig**	**57,1ml**
E**DTA**	**50mM**

Subsequently the methylated template DNA is digested by DpnI, which only happens after multiplying the bacteria-count, to obtain a pure PCR product. The wildtype DNA is removed by digestion of the DNA with 1µl Dpn1 for 1 hour at 37°C.

3.2 Transformation of competent E.Coli

After PCR and DpnI digest, the plasmid is transformed into competent E. Coli cells. The E.coli are taken from the freezer (-80°C) and defrosted on ice. Approximately 1µl of the digested DNA, depending on the intensity of the band on the Agarose-gel, is added and it is left on ice for another 20 minutes. Afterwards, they are heat shocked for 2 minutes at 42°C. 250µl of warm LB medium are added and shaken for one hour at 37°C. Finally, it is plated on the corresponding petri dishes (Ampicillin or Kanamycin, depending on the resistance of the plasmids). As a vector pcDNA3.1 V5 His TOPO by the company Clontech was used (seen in Figure 8).

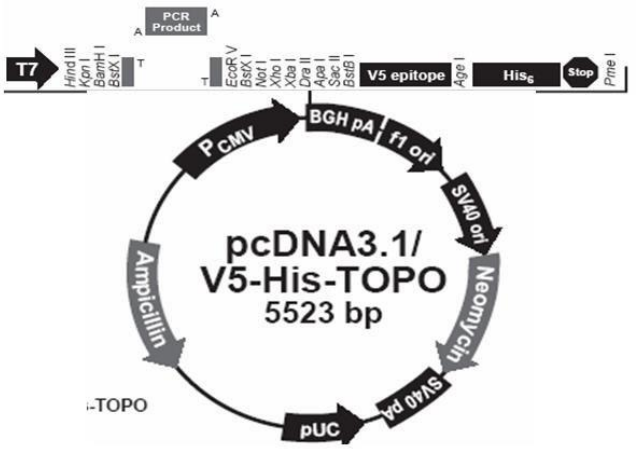

Figure 8: ***Backbone plasmid used for subcloning Orai1 cDNA and inserting point mutations***

3.3 Mini preparation – DNA purification

Material: PureYield^{TM} Plasmid Miniprep System (Promega)

Lysate Preparation

A colony is picked off a petri dish and left to grow in 3ml of medium and either Ampicillin resistance (1:1000) or Kanamycin (1:500). 100µl of Cell Lysis Buffer (Blue) are added to 600µl of the bacterial culture and the solution is mixed by inverting the tube six times. Then 350µl of cold (4-8°C) Neutralization Solution are added and the solution is mixed

thoroughly by inverting. The mixture is then centrifuged at maximum speed in a microcentrifuge for three minutes. Then the supernatant (about 900µl) is transferred to a PureYield™ Minicolumn without disturbing the cell debris pellet. The minicolumn is placed into a collection tube and centrifuged again at maximum speed for 15 seconds. The flow through is discarded and the minicolumn is placed into the same collection tube again.

Washing

200µl of Endotoxin Removal Wash (ERB) are added to the minicolumn. It is centrifuged at maximum speed in a microcentrifuge for 15 seconds. Afterwards 400µl of Column Wash Solution (CWC) are added to the minicolumn and it is again centrifuged at maximum speed for 30 seconds.

Elute

The minicolumn is transferred to a clean 1.5ml microcentrifuge tube, then 60µl of nuclease-free water are added directly to the minicolumn matrix and left to stand for 1 minute at room temperature. It is then centrifuged for 15 seconds to elute the plasmid DNA. The microcentrifuge tube is capped and the eluted plasmid DNA is stored at -20°C.

The DNA concentration is then checked via Nanodrop device (Thermo Scientifc) and 15µl are put into an extra tube and sent in for further sequencing (Eurofins Genomics).

3.4 Midi preparation – Increasing DNA amount

If the sequence is correct, a DNA Midi-Preparation Is carried out to achieve higher amounts of DNA.

Material: PureYield™ Plasmid Midiprep System (Promega)

Glycerol-stock

335µl of Glycerol and 665µl of the bacterial suspension are mixed and stored at -80˚C for later use.

Lysate and Precipitation

50ml medium are put in an Erlenmeyer flask. 50µl of Ampicillin resistance are added (or 100µl of Kanamycin). Then about 10µl of a glycerol-stock are added or scraped from the

plate with a pipette tip and placed inside the flask (with the tip!). It is then left over night at 37°C while being shaken.

DNA purification with vacuum

The blue column (Clearing Column) is placed inside the white column (Binding Column). The combined columns are placed into the vacuum station. The lysate is centrifuged, then put inside the clearing column and left in there for two to three minutes. The vacuum is turned on until the lysate has been completely run through. The blue column is then discarded. The vacuum is then turned on again and 5ml of Endotoxin Removal Wash are pulled through. Then 20ml of Column Wash Solution is pulled through the column. The vacuum is continued for another 30-60 seconds before it is turned off. The binding column is then removed from the vacuum station and the tip tapped on a paper towel to remove ethanol residue. It is then placed onto a new 1,5ml reactiontube. 600ml of nuclease-free-water are pipetted onto the binding-column, vacuum applied and left for five minutes. DNA is thus eluted from the filter into the tube, the concentration measured with- and can be stored at -20 for further experiments.

3.5 Transfection of HEK cells – Expression of Protein

Table 5: Reagents used for Transfection of HEK cells

Reagent	Volume
DMEM without additions	800µl
DNA	+10µg
Transfectionreagent (TransFectin, Biorad)	+10µl

Transfection

The materials seen in Table 5 are mixed and incubated for 20 minutes at room temperature. Then it is added dropwise onto the cells seeded in petri dishes. The cells are incubated at 37˚C with 5% CO_2 and in a humified atmosphere and grown for 2 days before transfection. Experiments are carried out 16-24 hours after transfection.

3.6 Protein Purification and Crosslinking

After 16-24 hours of incubation, the HEK 293 cells can be lysed. The first medium is discarded and the cells are rinsed off the bottom of the Petri dish with 1mL HBSS+1mM EDTA buffer. The solution is centrifuged for 1min at 4600rpm. The supernatant is discarded and the pellet resuspended in 1ml HBSS+1mM EDTA buffer, followed by centrifugation for 1min at 4600rpm.

This washing step is then repeated. After centrifugation the pellet is resuspended in 500µl Lysis Buffer, mixed with 15µl Protease Inhibitor and incubated on ice for 15 minutes. Then the solution is pulled up and down in a syringe (diameter 0.4x20mm) for 5 times. Next the solution is centrifuged for 10min at 4600rpm. The supernatant is now stored at -20°C. An aliquot of 20µl is treated with 5µl CuP-solution for 5min, then the reaction is stopped by addition of 5µl Quenching solution. To load the sample on the 12% SDS-page it has to be denatured with 10µl Laemmli buffer for 10min at 55°C.

3.7 SDS-Page and Western Blot

The 12% gels are prepared using the chemicals and amounts seen in Table 6 and Table 7. First the running gel is prepared and inserted into the gel-mold, after some time (around 20-30 minutes) the gel is polymerized and the stacking gel can be added.

Table 6: Chemicals and the corresponding amounts for preparation of the running gel.

12% Running Gel	For 2 gels (12ml)	4 gels (24ml)
Acrylamid/bis-acrylamid	4.8ml	9.6ml
Tris 1.5M pH 8.8	3.0ml	6.0ml
SDS 10%	120µl	240µl
APS (500mg/ml)	90µl	180µl
Water	3.86ml	7.72ml
TEMED	6µl	12µl

Table 7: Chemicals and the corresponding amounts for preparation of the stacking gel.

Stacking Gel	2 Gels (5ml)	4 gels (10ml)
Acrylamid/bis-acrylamid	0.66ml	1.32ml
Tris 0.5M pH 6.8	1.25ml	2.5ml
SDS 10%	50µl	100µl
APS (500mg/ml)	30µl	60µl
Water	2.99ml	5.98ml
TEMED	5µl	10µl

TEMED and APS are pipetted last because they can cause premature polymerisation. 21µl of sample is then mixed with 7µl Laemmli buffer and heated at 55˚C for 10min before loading on the gel. The SDS-page is run at 150V for about 1h 15min. For size comparison a protein size standard was used (Protein precision Plus, Biorad).

Western Blot

The stacking gel and the running gel are separated, then the running gel is placed in a transfer buffer. The membrane is cut into shape and first put into MetOH, afterwards in MilliQ water for a few minutes and then also submerged into the transfer buffer. A sponge is placed onto both sides of the western blot cassette, with some sheets of filter paper on top that had also been previously soaked in the transfer buffer. The running gel and the membrane are carefully placed in between the filter papers and the cassette is closed and placed into the instrument filled with transfer buffer. The western blot is then run for 1h 30 minutes.

3.8 Immunodetection

After blotting, the membrane is carefully removed from the cassette and put into a blocking solution (5% powdered milk dissolved in 1x TBST) for two hours, to prevent antibodies from binding to the membrane. The membrane is then washed with MilliQ water a few times. Afterwards, the membrane is submerged in Primary Antibody Solution for which Rabbit anti-Orai1 (1:2000) was used and shaken for one hour at room temperature. After washing it three times by shaking it in fresh TBST for 10 minutes, the membrane is placed in Horseradish peroxidase (HRP) Anti-Rabbit Secondary Antibody Solution (1:5000) and incubated on the shaker for one hour. At last, the membrane is again washed with TBST three times for 10 minutes.

1ml luminol and 1ml hydrogenperoxide were poured over the membrane and it was placed inside a hypercasette, with which it was taken inside a dark room. There, a photo-film was cut into the right size and placed onto the membrane inside the closed hypercasette for one minute. The film was developed using a Developing solution for 40 seconds and afterwards a Fixing solution for a few seconds. Then the film was shortely washed in MilliQ water and the marker-bands were labelled for further analysis.

4. Results

Among the mutations that we used for crosslinking was the F99C Mutation, which can be seen in Figure 9. For Translation of DNA into protein sequences the ExPAsy translation tool was used. For alignment with the wildtype Orai1 (PuBMed Acc. NM_032790.3) Clustal Omega < Multiple Sequence Alignment < EMBL-EBI was used (Figure 10).

```
> ANSGA H171Y F99C 3_T7 -- unclipped
ACCAGAAACTGTTAAGCTTGGTACCACATGAGCCTCAACGAGCACTCCATGCAGGCGCTG
TCCTGGCGCAAGCTCTACTTGAGCCGCGCCAAGCTTAAAGCCTCCAGCCGGACCTCGGCT
CTGCTCTCCGGCTGCGCCATGGTGGCAATGGTGGAGGTGCAGCTGGACGCTGACCACGAC
TACCCACCGGGGCTGCTCATCGCCTTCAGTGCCGTCACCACAGTGCTGGTGGCTGTGCAC
CTGTTTGCGCTCATGATCAGCACCGTCATCCTGCCCAACATCGAGGCGGTGAGCAACGTG
CACAATCTCAACTCGGTCAAGGAGTCCCCCCATGAGCGCATGCACCGCTATATCGAGCTG
GCCTGGGCCTTCTCCACCGTCATCGGCACGCTGCTCTTCCTAGCTGAGGTGGTGCTGCTC
GTCTGGGTCAAGTTCTTGCCCCTCAAGAAGCAGCCAGGCCAGCCAAGGCCCACCAGCAAG
CCCCCCGCCAGTGGCGCAGCAGCCGCAGTCAGCACCAGCGGCATCACCCCGGGCCAGGCA
GCTGCCATCGCCTCGACCACCATCATGGTGCCCTTCGGCCTGATCTTTATCGTCTTCGCC
GTCCACTTCTACCGCTCAGCGAATAGCGGTGCGACTGACCGACAGTTCCAGGAGCTCAAC
GAGCTGGCGGAGTTTGCCCGCTTACAGGACCAGCTGGACCACACAGAGGGGACCACCCCCTG
ACGCCCGGCAGCCACTATGCCTAGTCTAGAGGGCCCGCGGTTCGAAGGTAAGCCTATCCC
TAACCCTCTCCTCGGTCTCGATTCTACGCGTACCGGTCATCATCACCATCACCATTGAGT
TTAAACCCGCTGATCAGCCTCGACTGTGCCTTCTAGTTGCCAGCCATCTGTTGTTTGCCC
CTCCCCCGTGCCTTCCTTGACCCTGGAAGGTGCCACTCCCACTGTCCTTTCCTAATAAAA
TGAGGAAATTGCATCGCATTGTCTGAGTAGGTGTCATCTATCTGGGGGGGGGGGGGTGGG
GAAGAAAGCAAGGGGGAGGATTGGGAAGAAATAAAAGATGTTGGGGACCGGTTGGCTCTA
GGCTTCCAGCCGAAAGAACGCTGGGGCTCAGGGGTTCCCACGGCCAGGCCGGGCTTA
```

Figure 9: ***Sequencing result of a pcDNA3.1 plasmid containing hOrai1 and the desired F99C mutation***

```
ANSGAF99C       ---MSLNEHSMQALSWRKLYLSRAKLKASSRTSALLSGCAMVAMVEVQLDADHDYPPGLL  57
Orai1WT         SEVMSLNEHSMQALSWRKLYLSRAKLKASSRTSALLSGFAMVAMVEVQLDADHDYPPGLL  120
                   ********************************** ********************

ANSGAF99C       IAFSAVTTVLVAVHLFALMISTVILPNIEAVSNVHNLNSVKESPHERMHRYIELAWAFST  117
Orai1WT         IAFSACTTVLVAVHLFALMISTCILPNIEAVSNVHNLNSVKESPHERMHRHIELAWAFST  180
                ***** *************** *************************:*********

ANSGAF99C       VIGTLLFLAEVVLLVWVKFLPLKKQPGQPRPTSKPPASGAAAAVSTSGITPGQAAAIAST  177
Orai1WT         VIGTLLFLAEVVLLCWVKFLPLKKQPGQPRPTSKPPASGAAANVSTSGITPGQAAAIAST  240
                ************* ************************* ****************

ANSGAF99C       TIMVPFGLIFIVFAVHFYRSANSGATDRQFQELNELAEFARLQDQLDHRGDHPLTPGSHY  237
Orai1WT         TIMVPFGLIFIVFAVHFYRSLVSHKTDRQFQELNELAEFARLQDQLDHRGDHPLTPGSHY  300
                ******************  *  *********************************

ANSGAF99C       A 238
Orai1WT         A 301
                *
```

Figure 10: ***Alignment of ANSGA F99C with the wildtype Orai1. H171Y and F99C are shown in yellow, ANSGA is shown in grey.***

The endogenous cysteines (C126,143,195V) as well as the glycosylation site at N223 (N223A) were removed for a better outcome in the protein analysis.

The proteins that were separated by size via SDS-page were examined via kDa bands on the chemiluminescence detection of the membrane. The Orai subunit, forming hexameric structures consist of three dimers, which ensure the activation of the channel. The Orai1 dimer is observed around the 50 kDa mark, when being examined via western blot. The inactive monomer is found at 25 kDa, with about half of the dimers' molecular weight.

Calculation of Molecular weight (MW):

$$\text{mw} = \frac{Amino\ acids\ Orai1 * verage\ molecular\ weight\ of\ amino\ acid}{1000} = \frac{301 * 110\ Da}{1000} = 33.11 Da$$

4.1 Chemiluminescence Detection of the Membrane

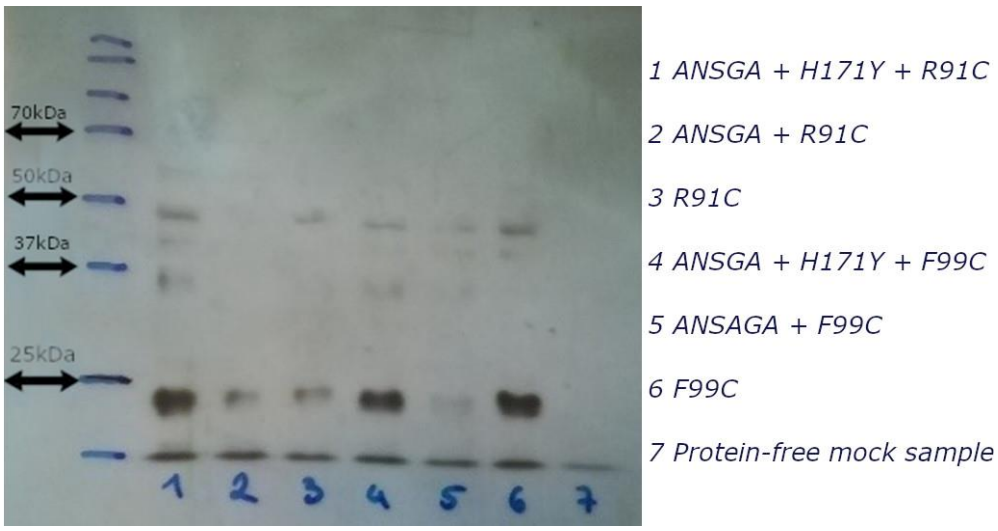

Figure 11: ***Chemiluminescence detection of Orai protein Structures via SDS page. Separation of different mutation types and combinations by size.***

In Figure 11 it can be seen for all examples except for the seventh, which was the protein-free mock sample including only the used reagents and the loading dye on the SDS-page, that a clearly visible band at 25 kDa appeared, indicating the monomer structure of Orai in the resting state. Another band can be observed at 50 kDa in all samples except in number 2, showing the activated dimeric structure.

4.1.1 Sample number 1

Continuous pore opening has been deactivated by combination of the ANSGA mutation with H171Y and R91C in Orai, which can be seen by the visible band at 50 kDa.

4.1.2 Sample number 2

No band is visible at 50 kDa, showing that only Orai1 monomers are present and therefore an opening of the channel. The ANSGA mutation combined with the non- polar cysteine residue on position 91 does not result in a mutation.

4.1.3 Sample number 3

A clearly visible band is present at the 50 kDa band, showing no channel activation by the mutation on the residue 91 from an acidic to a non-polar, uncharged amino acid.

4.1.4 Sample number 4

No continuous channel activity has been achieved by the combination of the ANSGA mutation with an uncharged amine acid at position 171 and F99C.

4.1.5 Sample number 5

The ANSGA mutation combined with the Phenylalanine, which has been exchanged for a Cysteine at position 99 did not lead to a full activation of the channel thus still showing a band at 50 kDa.

4.1.6 Sample number 6

A band can be seen at 50 kDa, showing that the F99C mutation without any further additions also leads to a deactivation of the channel.

4.2 Chemiluminescence Detection of the Membrane

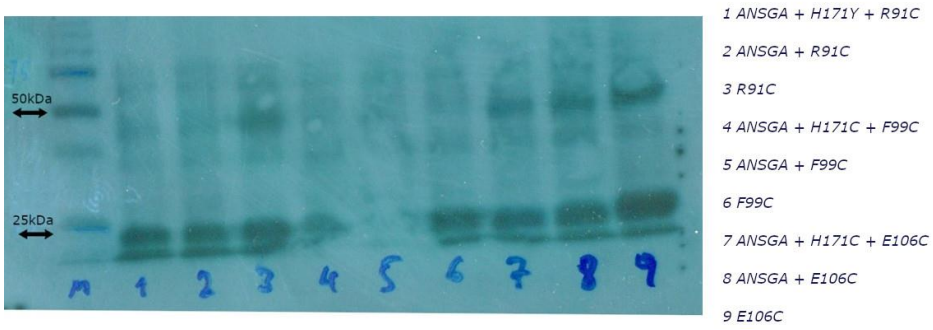

Figure 12: ***Chemiluminescence detection of Orai protein Structures via SDS page. Separation of different mutation types and combinations by size. Further results.***

4.2.1 Sample number 1

When combining R91C, ANSGA and H171Y the result is very similar to sample number two, showing that the addition of the H171Y mutation does not significantly change the structure of the pore.

4.2.2 Sample number 2

When combining R91C and ANSGA the band at 50 kDa indicates that the dimer is weaker than in sample number three. Less dimers have been formed, displaying that the R91C sidechains in the constitutive opened Orai1 channel are remote from another. The pore is less narrow as in a fully closed channel.

4.2.3 Sample number 3

A clearly visible monomer band can be seen for R91C, but also a relatively strong dimer, indicating that R91C in hexameric Orai1 channels are in close proximity.

4.2.4 Sample number 4

Combining F99C with ANSGA and H171Y does not lead to a band at 50 kDa, showing that there is no deactivation of the channel and only Orai1 monomers are present.

4.2.5 Sample number 5

No visible bands are shown at 25kDa and 50kDa for the combination of F99C and ANSGA.

4.2.6 Sample number 6

Only a band at 25kDa is visible for the Phenylalanine mutation at position 99, indicating an activated state of the channel.

4.2.7. Sample number 7

E106C in combination with ANSGA and H171Y led to bands at 25kDa as well as 50kDa, indicating a permanent closing of the channel.

4.2.8. Sample number 8

When combining the glutamic acid mutation on position 106 with ANSGA, also both bands can be detected.

4.2.9 Sample number 9

The band at 50kDa for only the E106C is very prominent, showing that the mutation itself does not lead to an activation of the channel.

4.3 Chemiluminescence Detection of the Membrane

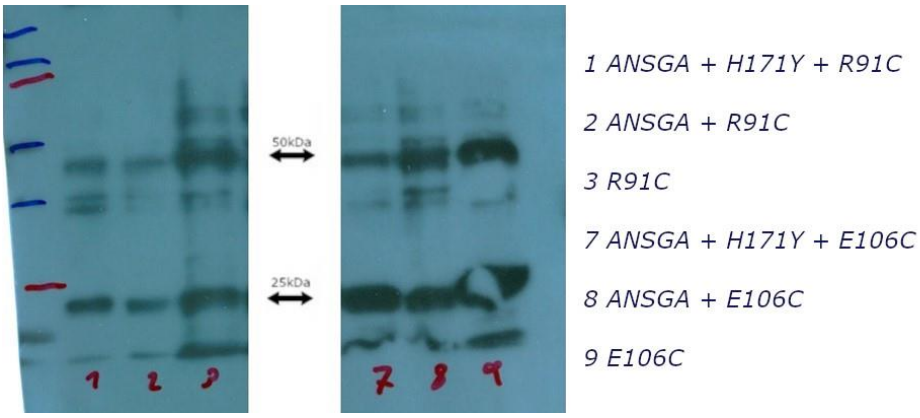

Figure 13: ***Chemiluminescence detection of Orai protein Structures via SDS page. Separation of different mutation types and combinations by size. Further results***.

4.3.1 Sample number 1

The combination of R91C, ANSGA and H171Y has been tested a third time, there is a clear distinction from sample number two without the H171Y mutation, showing a stronger band at 50kDa.

4.3.2 Sample number 2

Combining ANSGA and R91C shows a weaker band at 50kDa then when in combination with H171Y, thus showing that there is less dimerization.

4.3.3 Sample number 3

A very strong band is visible for R91C in Orai1, showing a strong dimerization and thus no activation of the channel.

4.3.4 Sample number 7

ANSGA, H171Y and the Glutamic acid that has been exchanged for a Cysteine at residue 106 combined in Orai1 show a strong band at 50kDa.

4.3.5 Sample number 8

An even stronger band at 50kDa can be seen for the combination of E106C and ANSGA, which is contrary to the assumption that ANSGA leads to an activation of the channel.

4.3.6 Sample number 9

Very strong bands at 25kDa and 50kDa can be seen for the E106 mutation in Orai1 without any further additions.

4.4 Chemiluminescence Detection of the Membrane

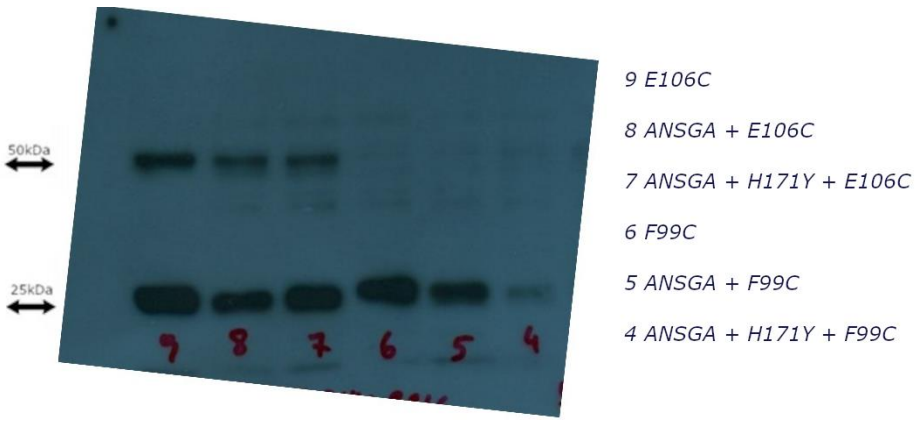

Figure 14: ***Chemiluminescence detection of Orai protein structures via SDS page. Separation of different mutation types and combinations by size. Further results.***

The band intensities on the membrane in Figure 14 were analysed using the program ImageJ (NIH). The corresponding results are shown in Figure 15. This way of evaluation has only been done for the last membrane, since it had the best outcome on band visibility. The results show the lowest degree of dimerisation for Sample nr. 7 (ANSGA + H171Y + E106C), thus showing that the amino acids in the channel are furthest apart. The other two samples are approximately identical.

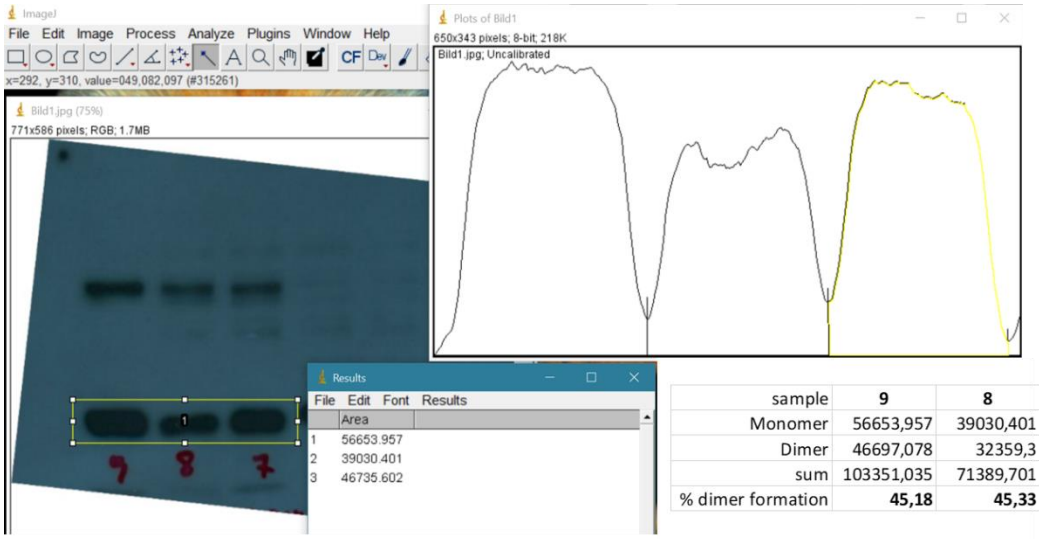

sample	9	8	7
Monomer	56653,957	39030,401	46735,602
Dimer	46697,078	32359,3	33390,329
sum	103351,035	71389,701	80125,931
% dimer formation	**45,18**	**45,33**	**41,67**

Figure 15: ***Schematic analysis of crosslinking patterns with the program ImageJ.***

4.4.1 Samples number 4, 5 and 6

All samples containing the F99C mutation (4,5,6) do not show crosslinking of cysteine residues to dimers. This may be explained by a too high distance between the sulfur atoms to crosslink.

4.4.2 Samples number 9

All samples show pronounced dimer formation. This assumes that the residue E106 is in close proximity to other E106 residues in the hexameric channel conformation. Adding the ANSGA mutation (E106C+ANSGA) does not seem to further enhance dimer formation indicating that adding the constitutively open ANSGA mutant does not influence the E106 residue.

Combining the E106C-ANSGA mutant with H171Y seems to partially reverse that effect. Dimer formation decreases, pointing to a dilation at that locus within the channel.

5. Discussion & Outlook

Introducing the ANSGA mutation into an Orai1 protein switches the channel in a constitutively open one. (Lunz, V., Romanin, C., & Frischauf, I., 2019*)* Within this thesis, it had been tested via cysteine-crosslinking, whether the mutation H171Y, believed to act as break-mutation (unpublished data), causes a change in the pore structure and thus a blockage of the Ca^{2+} flux. Therefore, we introduced several cysteine-mutations of pore-lining amino acids into a Orai1 ANSGA + H171Y background. Crosslinking of cysteines can be visualized as dimer band on SDS PAGE and indicates close proximity of the respective residues within the hexameric channel complex. Monomers, respectively, point to increased distance of residues, preventing cysteine-crosslinking. Such as was also shown by Frischauf and her team by working with wildtype Orai1 and Prai1-H134A channels, where they examined differences in the pore structures and successfully achieved crosslinking between the cysteines at the TM1 residues and thus proving their close proximity. Between cysteine free combinations only monomers formed, while for single cysteine substitutions both, monomers and dimers were found. (Frischauf et al., 2017)

Combining and analyzing the blots carried out during this thesis, we can make the following statements:

- The most pronounced effect can be seen at position R91C. Within the closed Orai channel (R91C alone), R91 residues are close to each other and form disulfide bridges resulting in dimer bands. Combining the R91C mutation with ANSGA (switching the channel into an open conformation), leads to reduced dimer formation which indicates that R91 residues move further apart in the open channel configuration. By addition of H171Y to the ANSGA+R91C Orai1 construct, we could observe an increased dimer formation again. This is in line with our hypothesis that H171Y acts a break mutation, reversing the constitutive activity caused by the ANSGA mutant.
- For the other tested pore-lining residues (F99C and E106C) we could not observe such an effect. There are no differences seen in crosslinking-patterns, in either the single cysteine-substitution or in the combination with ANSGA or ANSGA+H171Y. One possible explanation is that these pore-lining residues are not affected during the process of channel opening. This is plausible as the E106 residue acts as selectivity filter of the channel and is located at the upper,

extracellular mouth of the CRAC channel. Upon channel opening, the selectivity of the channel should not change under physiological conditions.

So far, we can conclude that the Orai1-ANSGA mutant causes a change in dimerization of the CRAC channel, which also conclude the findings of Zhou Y., et al. 2016, which examined Orai1 channels with mutations of, among others, Valine and Leucine in combination with Histidine and/or Lysine in HEK cells and found that the mutations in the nexus region resulted in a store-independent constitutive channel activity. (Zhou Y., et al. 2016)

The constitutive activity of the Orai1-ANSGA mutant containing substitutions within the hinge region can be overruled by MTR-LoF point mutations, independent of their position relative to each other, which was tested with combinations of Orai1-ANSGA and different mutations such as with H134W and A235W by Tiffner A., et al. 2021. While this thesis investigated the Orai1-ANSGA mutation in combination with H171Y and another mutation, they combined the Orai1-ANSGA mutant with the MTR-GoF point mutation V181F, Orai1 H134A A235W/S239W. Their results showed reduced or eliminated channel-function in the presence of STIM1. (Tiffner A., et al. 2021)

Clearly, there are more experiments needed to confirm the observed effects.

6. Literature

Baker B. S., Young G. T., Soubrane C. H., Stephens G. J., Stephens E. B., Patel M. K. *Ion Channels. Conn's Translational Neuroscience*, Chapter 2: 11-43, (2017).

Berridge, M.J., Bootman, M.D., & Roderick, H.L. (2003). *Calcium signalling; dynamics, homeostasis and remodelling. Nature Reviews Molecular Cell* Biology, 4(7), 517-529.

Clapham, D.E. (2007). *Calcium Signaling. Cell*, 131(6), 1047-1058.

Di Resta C., Becchetti A. (2010) *Introduction to ion channels*. *In: Becchetti A., Arcangeli A. (eds) Integrins and Ion Channels. Advances in Experimental Medicine and Biology*, vol 674. Springer, New York, NY

Frischauf, I., Litviňuková, M., Schober R., et al. (2017) *Transmembrane helix connectivity in Orai1 controls two gates for calcium-dependent transcription.* Science Signaling, Vol. 10, Issue 507, eaao0358

Lunz, V., Romanin, C., & Frischauf, I. (2019*). STIM1 activation of ORAI1*. *Cell Calcium*, 77, 29-38.

Misceo, D., Holmgren, A., Louch, W.E., Holme, P.A., Mizobuchi, M., Morales, R.J., et al. (2014). *A Dominant STIM1 Mutation Causes Stormorken Syndrome. Human Mutation*, 35(5), 556-564.

Möhm, .J, Chevessier, F., De Paula, A. M., Koch, C., Attarian, S., Feger, C., et al. (2013) *Constitutive Activation of the Calcium Sensor STIM1 Causes Tubular-Aggregate Myopathy. The American Journal of Human Genetics.* 92(2), 271-278.

Nowycky, M. C. (2002). *Intracellular calcium signalling.* Journal of Cell Science, 115(19), 3715-3716.

Parekh, A.B. (2010). *Store-operated CRAC channels: function in health and disease. Nature Reviews Drug Discovery*, 9(5), 399-410.

Prakriya, M. (2009). *The molecular physiology of CRAC channels. Immunological Reviews*, 231(1), 88-98.

Rosado, J.A., Diez, R., Smani, T., & Jardin, I. (2016). *STIM and ORAI1 Variants in Store-Operated Calcium Entry. Frontiers in Pharmacology, 6.*

Sallinger, M., Berlansky, S., & Frischauf, I. (2020). *Orai channels: keyplayers in Ca^{2+} homeostasis.* Current Opinion in Physiology 2020, 17:42–49

Snutch, T.P., & Reiner, P.B. (1992). *Ca^{2+} channels: diversity of form and function. Current Opinion in Neurobiology*, 2(3), 247-253.

Tiffner, A., Schober R., Höglinger, C., et al. *CRAC channel opening is determined by a series ofOrai1 gating checkpoints in the transmembrane andcytosolic regions.* J. Biol. Chem. (2021) 296 100224

Zhou, Y., Cai, X., Loktionova, N. *et al. The STIM1-binding site nexus remotely controls Orai1 channel gating.* Nat Commun 7, 13725 (2016).

Zhou Y., Cai X., Nwokonko R.M., Loktionova N.A., Wang Y., Grill D.L. *The STIM-Orai coupling interface and gating of the Orai1 channel. Cell Calcium.* 2017;61:1-7